PROCEEDINGS OF SCIENCE

Hybrid static potentials and gluelumps on $N_f = 3 + 1$ ensembles

Roman Höllwieser,[a,*] **Francesco Knechtli,**[a] **Tomasz Korzec,**[a] **Michael Peardon,**[b] **Laura Struckmeier**[a] **and Juan Andrés Urrea-Niño**[a]

[a] *Department of Physics, University of Wuppertal, Gaußstrasse 20, 42119 Germany*
[b] *School of Mathematics, Trinity College Dublin, Ireland*

E-mail: hoellwieser@uni-wuppertal.de

QCD permits the existence of hybrid mesons that are made up of both quarks and gluons, including exotic states, i.e., quantum numbers prohibited for pure quark-antiquark states, with possible candidates found in experiments. We present static hybrid potentials measured via Laplace trial states together with static-light meson thresholds on $N_f = 3 + 1$ dynamical fermion ensembles with 420 MeV pions. Furthermore, we measure corresponding gluelump masses which refer to the $R \to 0$ limit of the hybrid potentials and are essential input parameters for effective models to describe hybrid mesons.

The 41th International Symposium on Lattice Field Theory (Lattice 2024)
July 28th - August 3rd, 2024
University of Liverpool

*Speaker

© Copyright owned by the author(s) under the terms of the Creative Commons Attribution-NonCommercial-NoDerivatives 4.0 International License (CC BY-NC-ND 4.0).

arXiv:2501.15670v1 [hep-lat] 26 Jan 2025

1. Introduction

Static-hybrid quark anti-quark potentials represent a promising frontier in the quest to decipher the strong force's intricacies. These potentials offer a unique perspective on meson behavior, bridging the gap between traditional quark models and lattice QCD simulations [1]. In particular, XYZ states have posed significant challenges to our understanding of hadron spectroscopy. These states do not fit neatly into the quark model, and their properties pose questions about their internal structure and how they relate to QCD [2, 3]. Static-hybrid mesons could provide a theoretical framework to help explain or categorize some XYZ states [4, 5]. At small static source separation r, the hybrid potentials form multiplets associated with *gluelumps*, which are energy levels of QCD in the presence of a color-octet source [6, 7]. We show how to construct new hybrid static operators with trial states formed by eigenvector components of the covariant lattice Laplace operator, where the gluonic excitations are realized via covariant derivatives of individual eigenvectors. For the computation of gluelump masses, we follow a classical method [8–11] refined by using an extended basis of spatial loop shape correlations recently introduced in [12] for glueball calculations.

2. Methods

In [13, 14] we show that we can replace the spatial Wilson line in classical Wilson loops by eigenvector pairs $v_i(\vec{x})v_i(\vec{y})$ of the three-dimensional gauge-covariant lattice Laplace operator to build so-called *Laplace trial state correlators*. We can also write the latter as the spatial correlation of static perambulators $\tau_{ij}(\vec{y},t_0,t_1) = v_i^\dagger(\vec{y},t_0)U_t(\vec{y},t_0,t_1)v_j(\vec{y},t_1)$, and $\bar{\tau}_{ij}(\vec{x},t_0,t_1)$, where $\vec{x}$ and $\vec{y} = \vec{x} + \vec{r}$ denote the location of the static sources. Practically, these static quark line operators are computed first and can be correlated at arbitrary distances, which allows to compute on- and off-axis distances very easily.

In order to build hybrid Laplace trial states we introduce gluonic excitations via covariant derivatives of the Laplacian eigenvectors

$$\nabla_{\vec{k}} v(\vec{x}) = \frac{1}{2}[U_k(\vec{x})v(\vec{x}+\hat{k}) - U_k^\dagger(\vec{x}-\hat{k})v(\vec{x}-\hat{k})].$$

We extract hybrid static potentials from the correlation functions

$$C_{\Sigma_g^+}(R,T) = \sum_{\vec{x},t_0,i,j} \left\langle \mathrm{Tr}\big[\tau_{ij}(\vec{y},t_0,t_1)\rho^2(\lambda_j)\tau_{ji}(\vec{x},t_1,t_0)\rho^2(\lambda_i)\big]\right\rangle =$$
$$\sum_{\vec{x},t_0,i,j} \left\langle \mathrm{Tr}\big[U_t(\vec{y};t_0,t_1)\rho^2(\lambda_j)v_j(\vec{y},t_1)v_j^\dagger(\vec{x},t_1)U_t^\dagger(\vec{x};t_0,t_1)\rho^2(\lambda_i)v_i(\vec{x},t_0)v_i^\dagger(\vec{y},t_0)\big]\right\rangle,$$

$$C_{\Sigma_{u/g}^+}(R,T) =$$
$$\sum_{\vec{x},t_0,i,j,\vec{k}||\vec{r}} \Big\langle \mathrm{Tr}\big[U_t(\vec{y};t_0,t_1)\rho^2(\lambda_j)\{[\nabla_{\vec{k}}v_j](\vec{y},t_1)v_j^\dagger(\vec{x},t_1) \pm v_j(\vec{y},t_1)[\nabla_{\vec{k}}v_j]^\dagger(\vec{x},t_1)\}$$
$$U_t^\dagger(\vec{x};t_0,t_1)\rho^2(\lambda_i)\{[\nabla_{\vec{k}}v_i](\vec{x},t_0)v_i^\dagger(\vec{y},t_0) \pm v_i(\vec{x},t_0)[\nabla_{\vec{k}}v_i]^\dagger(\vec{y},t_0)\}\big]\Big\rangle,$$

$$C_{\Pi_{u/g}}(R,T) =$$
$$\sum_{\vec{x},t_0,i,j,\vec{k}\perp\vec{r}} \Big\langle \mathrm{Tr}\big[U_t(\vec{y};t_0,t_1)\rho^2(\lambda_j)\{[\nabla_{\vec{k}}v_j](\vec{y},t_1)v_j^\dagger(\vec{x},t_1) \pm v_j(\vec{y},t_1)[\nabla_{\vec{k}}v_j]^\dagger(\vec{x},t_1)\}$$
$$U_t^\dagger(\vec{x};t_0,t_1)\rho^2(\lambda_i)\{[\nabla_{\vec{k}}v_i](\vec{x},t_0)v_i^\dagger(\vec{y},t_0) \pm v_i(\vec{x},t_0)[\nabla_{\vec{k}}v_i]^\dagger(\vec{y},t_0)\}\big]\Big\rangle,$$

where $R = |\vec{r}| = |\vec{y} - \vec{x}|$ and $T = |t_1 - t_0|$. We improve the overlap of the operator by introducing a set of Gaussian profile functions $\rho_k(\lambda_i) = e^{-\lambda_i^2/4\sigma_k^2}$ to give different weights to individual eigenmodes v_i according to their eigenvalues λ_i. We work with seven different Gaussian widths σ_k and construct a correlation matrix and solve a generalized eigenvalue problem (GEVP) using the pruned matrix to identify the optimal trial state profiles.

In the limit of the separation between the **3** and **3*** sources $r \to 0$, since $\mathbf{3} \otimes \mathbf{3}^* = \mathbf{1} \oplus \mathbf{8}$, their effect on the fields of QCD becomes more and more like that of a linear combination of a local color-singlet (**1**) source and a local color-octet (**8**) source. While a singlet state decouples from the temporal transporters within an $r = 0$ "Wilson loop", an octet state couples to a temporal Schwinger line in the adjoint representation. In the infinite mass limit, where spin can be neglected, the temporal transporter can be interpreted as the propagator of a static gluon, in analogy to fundamental lines representing a static quark. Hence, only the color-octet component acts as a local source of gluonic fields, restoring the rotational and the discrete symmetries of QCD in the limit $r \to 0$, approaching states with definite J^{PC} quantum numbers and with specific light-quark flavors. In pure $SU(3)$ gauge theory, a state with discrete energy bound to an **8** source is called a *gluelump* [6, 7, 15]. The spectrum of QCD in the presence of a static color-octet source can be calculated using lattice QCD up to an additive constant [8–10]. We compute gluelump masses from correlation functions of spatial Wilson loops transformed to the adjoint representation connected with an adjoint static line. We perform one HYP2 smearing step for temporal gauge links and three levels of APE smearing steps for spatial links, building a correlation matrix from different levels being treated as a generalized eigenvalue problem (GEVP) [16]. We use $s = 1 \ldots 35$ different 3D loop shapes, denoted as $W_s(\vec{x}, t)$, starting at a spatial point $\vec{x}$ at fixed Euclidean time t, as introduced in [12, 17] for glueball operators. Parity is fixed by considering the sum (P=+1) or difference (P=-1) of each loop with its parity twin, *i.e.*, the loop under the action of a parity transformation. Charge conjugation symmetry is fixed by using $W_s^{P,C=\pm} = W_s^P \pm W_s^{P\,\dagger}$. Elements of the cubic group can act on $W_s^{PC}(\vec{x}, t)$, resulting in 24 loops which form a basis which generates the regular (or permutation) representation of the cubic group, not considering any degeneracies between loops. Therefore, there exist linear combinations of the 24 loops with projection coefficients transforming according to any of the five irreps of the cubic group $\Lambda \in \{A1, A2, E, T1, T2\}$, were we consider only one copy per irrep. The corresponding coefficients can be calculated via projection methods [18, 19] and differ from those for glueballs, since there is no sum over spatial points $\vec{x}$ and symmetries have to hold locally. We choose projection basis vectors containing no zeros to maximize the use of operators and sum over all loop shapes contributing to a specific irrep, which eliminates the shape index s in the final operators. The projection to the adjoint representation can be avoided by writing the correlator in terms of fundamental operators $W_{\Lambda^{PC}}(\vec{x}, t)$ and static lines $U_t(\vec{x}, t_0, t_1)$ [10, 11]

$$C_{\Lambda^{PC}}(t) = \sum_{\vec{x},t_0} \Big\{ \mathrm{Tr}[W_{\Lambda^{PC}}(\vec{x}, t_0) U_t(\vec{x}, t_0, t_0 + t) W^\dagger_{\Lambda^{PC}}(\vec{x}, t_0 + t) U_t^\dagger(\vec{x}, t_0, t_0 + t)] \quad (1)$$

$$- \mathrm{Tr}[W_{\Lambda^{PC}}(\vec{x}, t_0)] \mathrm{Tr}[W^\dagger_{\Lambda^{PC}}(\vec{x}, t_0 + t)]/3 \Big\} \quad (2)$$

We extract gluelump masses from exponential fits to the correlators containing a self-energy contribution $m_{self}(a)$ from adjoint color sources. The latter differs from the self-energy in the (hybrid)

static potentials $V_{self}(a)$, however, the two can be related via [8, 20–23]

$$m_{self}(a) = \frac{C_A}{C_F}\frac{V_{self}(a)}{2} = \frac{N^2}{N^2-1}V_{self}(a) > V_{self}(a), \tag{3}$$

with $C_A = N$ and $C_F = (N^2-1)/2N$ the quadratic Casimir invariants of the adjoint and fundamental representations of $SU(N)$. Since for $SU(3)$ the relative factor is close enough to one, we include the gluelump masses in the potential plots without additional shifts.

3. Ensembles

We work with one quenched ensemble (qE), an $N_f = 2$ ensemble (Em1) with two dynamical quarks of half the charm quark mass ($m_\pi = 2.2$ GeV), both of lattice size 48×24^3 and $N_f = 3+1$ ensembles with 788 MeV (A1h) and 406 MeV (A1) pions on 96×32^3 lattice volumes, as well as the latter pion mass also on a larger volume (A2, 128×48^3, $m_\pi = 409$ MeV) [24]. The 48×24^3 lattices have periodic boundary conditions while the $N_f = 3+1$ ensembles have open boundaries in temporal direction. They were all produced with the openQCD package [25] using the plaquette (qE,Em1) and Lüscher-Weisz gauge action (A1h,A1,A2). For the latter ($N_f = 3+1$) ensembles we use Wilson quarks with a non-perturbatively determined clover coefficient in a massive O(a) improvement scheme [26]. The bare gauge couplings $g_0^2 = 6/\beta$ and the hopping parameters, as well as the Sommer scale r_0/a [27], the flow scale t_0/a^2 [28] and corresponding lattice spacing (defined via the mass difference of h_c and η_c [24]) are given in table 1. All measurements were performed by our C+MPI based library that facilitates massively parallel QCD calculations. A total of N_{vec} eigenvectors of the 3D covariant Laplacian were calculated on each time-slice of the lattices. A total of 20 3D APE smearing [29] steps with $\alpha_{APE} = 0.5$ were applied on each gauge field before the eigenvector calculation so as to smooth the link variables that enter the Laplacian operator. When forming the correlations of the Laplace trial states, we apply one HYP2 smearing step with parameters $\alpha_1 = 1$, $\alpha_2 = 1$ and $\alpha_3 = 0.5$ to the temporal links [30–34], which corresponds to a particular choice of the static action. The error analysis in this work was done using the Γ method [35, 36] in a recent python implementation (pyerrors) [37] with automatic differentiation [38].

4. Results

We present gluelump masses measured on the full statistics on all ensembles. Since the lattice energies contain the unphysical self-energy Eq. (3), only mass differences have a continuum limit and we consider the mass differences with respect to the T^{+-} state, which happens to be the lowest state. We follow the ordering of low lying gluelumps as been established [8] and plot the masses against J^{PC} assuming the lowest spin contained in the O_h representation in figure 1 for various ensembles. The results on the two similar ensembles A1 and A2 only differing by their volumes are in perfect agreement with each other, hence we do not include the masses of A2 in this plot. It is also reassuring to see that E^{PC} and T_2^{PC} are consistent with each other for each PC, since they should couple to the same physical state ($J = 2$) in the continuum limit, hence we plot them with a slight offset next to each other in the corresponding 2^{PC} channel. We find the individual energies consistently increasing with decreasing pion mass.

ensemble	qE	Em1	A1h	A1	A2
volume	48×24^3	48×24^3	96×32^3	96×32^3	128×48^3
β	5.85	5.3	3.24	3.24	3.24
κ_l	-	-	0.13392	0.134407	0.134396
κ_c	-	0.13270	0.12834	0.12784	0.12798
m_π	-	2.2(1) GeV	788(6) MeV	406(3) MeV	409(1) MeV
r_0/a	4.2612(42)	4.2866(24)	7.278(27)	9.023(63)	8.998(54)
t_0/a^2	-	1.8477(3)	5.078(14)	7.438(32)	7.434(20)
a [fm]	0.0662(12)	0.0658(10)	0.0690(11)	0.05359(15)	0.05355(13)
N_{cfg}	6480	7098	4000	4000	2000
N^l_{vec}	-	-	200	100	100
N^l_{per}	-	-	2000	4000	2000
N^c_{vec}	-	200	200	200	-
N^c_{per}	-	1000	2000	4000	-

Table 1: Lattice, simulation and distillation (numbers of eigenvectors and perambulators for light and charm quarks) parameters of the ensembles qE (quenched), Em1, A1 heavy and A1 resp. A2 (light).

We show the hybrid static ground state potentials of $\Sigma_{g/u}$ and $\Pi_{g/u}$ and some excited states in figure 2 for Em1 and A2 ensembles. We plot the potentials relative to twice the static-light S-wave energy m_S and also mark the static light $P_{1/2}$ and $P_{3/2}$-wave energies $m_{P_{1/2}}$ and $m_{P_{3/2}}$. We see that for Em1 (and A1) expected string breaking distances of Σ_g and Π_u are just above half the spatial lattice extent, on A2 we could actually study hybrid string breaking. For on-axis separations the potential of $\Pi_{g/u}$ in the continuum representation can be obtained from the $E^\mp_1$ representation of D_{4h}. For off-axis separations (Em1 only) we technically do not have D_{4h}, but we can consider off-axis separations in a 2D plane only rather than the 3d volume, to be left with one orthogonal direction for the covariant derivatives, see also [39]. For Σ_u with derivatives along the separation axis we compute on-axis distances only. We include the lowest gluelump masses corresponding to the $R \to 0$ limit of the lowest hybrid potentials, also subtracting twice the static-light S-wave mass, which does not completely remove the self-energy contribution. Nevertheless, the limits look reasonable.

5. Conclusions & Outlook

We have computed gluelump spectra and hybrid static potentials $V_{\Lambda^\epsilon_\eta}(r)$ for $\Lambda^\epsilon_\eta = \Sigma_{g/u}$ and $\Pi_{g/u}$ states in SU(3) lattice gauge theory. For the computation of gluelump masses we use an extended basis of spatial loop shape correlations. Comparison of E and T_2 representations, both of which couple to $J = 2$ in the continuum limit, provides a cross-check on cutoff effects. For the hybrid static potentials we use alternative operators for a static quark-anti-quark pairs based on Laplacian eigenmodes, replacing traditional Wilson loops. Instead of "gluonic handles" (excitations) of the spatial Wilson lines we use symmetric, covariant derivatives of the Laplacian eigenvectors to form improved Laplace trial states by applying optimal profiles to give different weights to individual

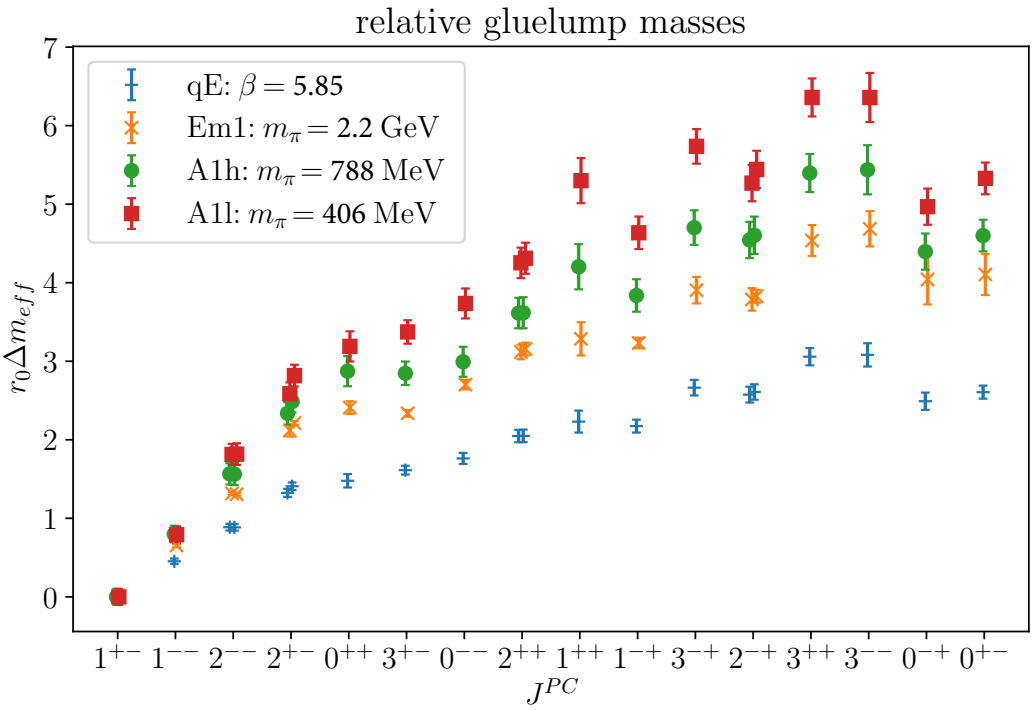

Figure 1: Relative gluelump masses $r_0 \Delta m_{eff} = r_0/a\ (\ am_{eff,\Lambda} - am_{eff,T1^{+-}}\ )$ on ensembles qE (quenched), Em1 (m_π = 2.2GeV), A1 heavy (m_π = 788 MeV) and A1 light (m_π = 406 MeV).

eigenvectors, derived from a generalized eigenvalue problem. A high resolution of the hybrid static potentials can be achieved as off-axis distances can easily be computed in the new approach. We present a hybrid static spectrum including excited states and show their optimal profiles which allow us to extract effective energies from reasonable effective mass plateaus. In the spectrum we also mark the string breaking thresholds from static-light S- and P-waves, on ensemble A2 we could actually study the string breaking of Σ_g and Π_u. The computation of (hybrid) static-light correlators using "perambulators" $v(t_1)D^{-1}v(t_2)$ from the distillation framework was presented in [40]. This allows us to put together the building blocks for string breaking in QCD, computing the mixing matrix including static and light quark propagators. The new methods can also be applied to tetra- and multi-quark potentials, which is the plan for future investigations.

Acknowledgements

The authors gratefully acknowledge the Gauss Centre for Supercomputing e.V. (www.gauss-centre.eu) for funding this project by providing computing time on the GCS Supercomputer SuperMUC-NG at Leibniz Supercomputing Centre (www.lrz.de). M.P. was supported by the European Union's Horizon 2020 research and innovation programme under grant agreement 824093 (STRONG-2020). The work is supported by the German Research Foundation (DFG) research unit FOR5269. The project received funding from the programme " Netzwerke 2021", an initiative of the Ministry of Culture and Science of the State of Northrhine Westphalia, in the NRW-FAIR network, funding code NW21-024-A (R.H.). We thank Abhishek Mohapatra, Nora Brambilla and Stefano Capitani for valuable discussions.

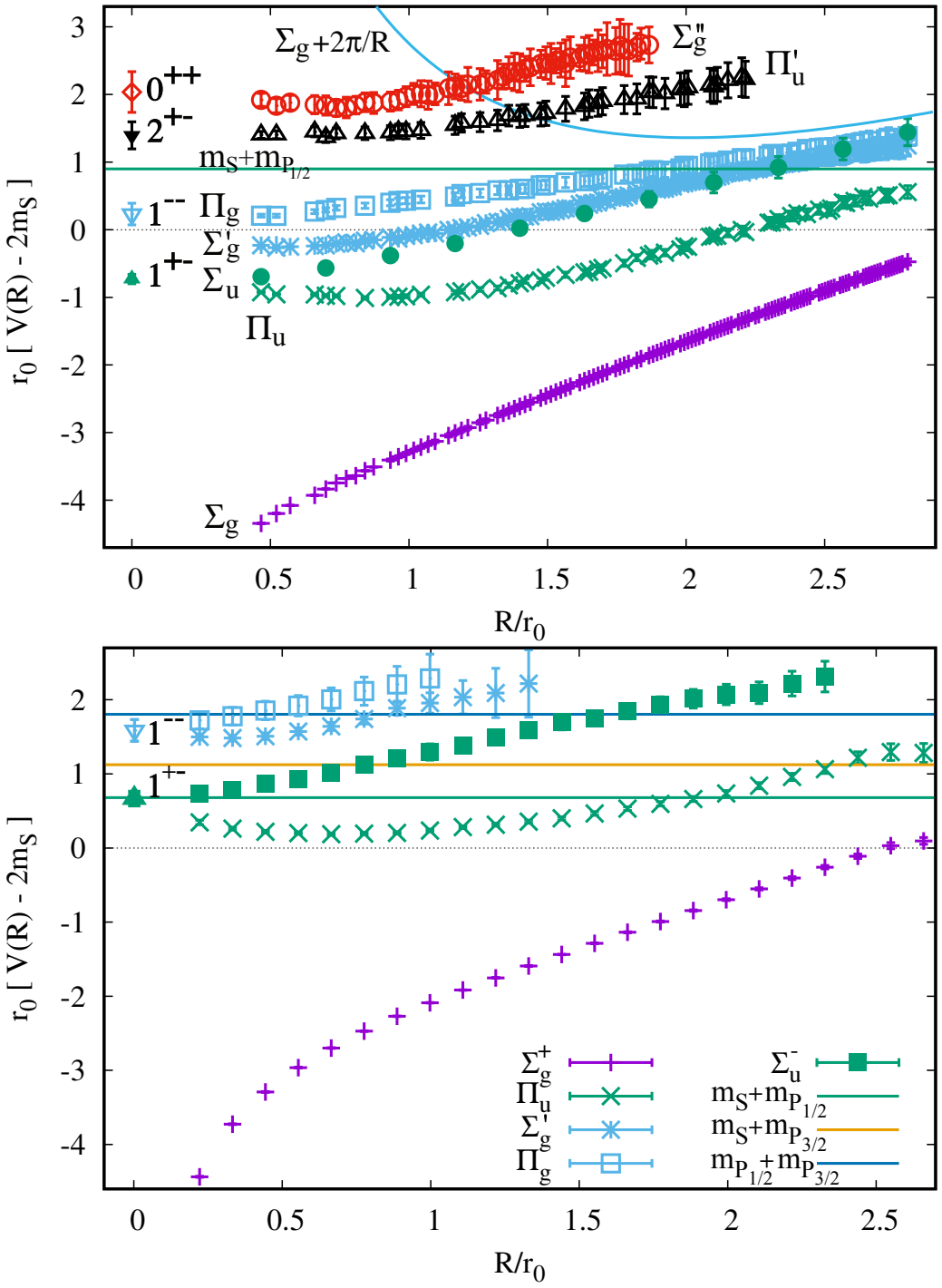

Figure 2: Hybrid static potentials and corresponding gluelumps on Em1 (top) and A2 (bottom) relative to twice the static-light S-wave mass m_S and the $P_{1/2}$-wave mass $m_{P_{1/2}}$. For A2 we also show the $P_{3/2}$-wave mass.

References

[1] J. J. Dudek, *Phenomenology of exotic hadrons - hybrid mesons and pentaquarks*. PhD thesis, Oxford U., Theor. Phys., 2004.

[2] E. S. Swanson, "XYZ States: Theory Overview," *AIP Conf. Proc.* **1735** no. 1, (2016) 020013, arXiv:1512.04853 [hep-ph].

[3] N. Brambilla, S. Eidelman, C. Hanhart, A. Nefediev, C.-P. Shen, C. E. Thomas, A. Vairo, and C.-Z. Yuan, "The XYZ states: experimental and theoretical status and perspectives," *Phys. Rept.* **873** (2020) 1–154, arXiv:1907.07583 [hep-ex].

[4] M. Berwein, N. Brambilla, A. Mohapatra, and A. Vairo, "One Born−Oppenheimer Effective Theory to rule them all: hybrids, tetraquarks, pentaquarks, doubly heavy baryons and quarkonium," arXiv:2408.04719 [hep-ph].

[5] S. Capitani, O. Philipsen, C. Reisinger, C. Riehl, and M. Wagner, "Precision computation of hybrid static potentials in SU(3) lattice gauge theory," *Phys. Rev. D* **99** no. 3, (2019) 034502, arXiv:1811.11046 [hep-lat].

[6] N. A. Campbell, I. H. Jorysz, and C. Michael, "The Adjoint Source Potential in SU(3) Lattice Gauge Theory," *Phys. Lett. B* **167** (1986) 91–93.

[7] I. H. Jorysz and C. Michael, "The Field Configurations of a Static Adjoint Source in SU(2) Lattice Gauge Theory," *Nucl. Phys. B* **302** (1988) 448–470.

[8] **UKQCD** Collaboration, M. Foster and C. Michael, "Hadrons with a heavy color adjoint particle," *Phys. Rev. D* **59** (1999) 094509, arXiv:hep-lat/9811010.

[9] K. Marsh and R. Lewis, "A lattice QCD study of generalized gluelumps," *Phys. Rev. D* **89** no. 1, (2014) 014502, arXiv:1309.1627 [hep-lat].

[10] J. Herr, C. Schlosser, and M. Wagner, "Gluelump masses and mass splittings from SU(3) lattice gauge theory," *Phys. Rev. D* **109** no. 3, (2024) 034516, arXiv:2306.09902 [hep-lat].

[11] J. Herr, "Computation of gluelump masses for hybrid static potentials in SU(3) lattice gauge theory using the multilevel algorithm," *MSc thesis at Goethe University Frankfurt* (2022) .

[12] L. Barca, S. Schaefer, F. Knechtli, J. A. Urrea-Niño, S. Martins, and M. Peardon, "Exponential error reduction for glueball calculations using a two-level algorithm in pure gauge theory," *Phys. Rev. D* **110** no. 5, (2024) 054515, arXiv:2406.12656 [hep-lat].

[13] R. Höllwieser, F. Knechtli, T. Korzec, M. Peardon, and J. A. Urrea-Niño, "Constructing static quark-antiquark creation operators from Laplacian eigenmodes," *Phys. Rev. D* **107** no. 3, (2023) 034511, arXiv:2212.08485 [hep-lat].

[14] R. Höllwieser, F. Knechtli, and M. Peardon, "The static energy of a quark-antiquark pair from Laplacian eigenmodes," *PoS* **LATTICE2022** (9, 2022) 060, arXiv:2209.01239 [hep-lat].

[15] F. Alasiri, E. Braaten, and A. Mohapatra, "Born-Oppenheimer Potentials for $SU(3)$ Gauge Theory," arXiv:2406.05123 [hep-ph].

[16] B. Blossier, M. Della Morte, G. von Hippel, T. Mendes, and R. Sommer, "On the generalized eigenvalue method for energies and matrix elements in lattice field theory," *JHEP* **04** (2009) 094, arXiv:0902.1265 [hep-lat].

[17] B. Berg and A. Billoire, "Glueball Spectroscopy in Four-Dimensional SU(3) Lattice Gauge Theory. 1.," *Nucl. Phys. B* **221** (1983) 109–140.

[18] H. Georgi, "Lie Algebras in Particle Physics: From Isospin to Unified Theories," *CRC Press* (2018) .

[19] P. R. Bunker and P. Jensen, "Molecular symmetry and spectroscopy," *NRC Press, Ottawa, ON, Canada, 2 edition* (1998) .

[20] G. S. Bali, "QCD forces and heavy quark bound states," *Phys. Rept.* **343** (2001) 1–136, arXiv:hep-ph/0001312.

[21] C. Bauer, G. S. Bali, and A. Pineda, "Compelling Evidence of Renormalons in QCD from High Order Perturbative Expansions," *Phys. Rev. Lett.* **108** (2012) 242002, arXiv:1111.3946 [hep-ph].

[22] G. S. Bali, C. Bauer, A. Pineda, and C. Torrero, "Perturbative expansion of the energy of static sources at large orders in four-dimensional SU(3) gauge theory," *Phys. Rev. D* **87** (2013) 094517, arXiv:1303.3279 [hep-lat].

[23] G. S. Bali, C. Bauer, and A. Pineda, "The static quark self-energy at $O(\alpha^2 0)$ in perturbation theory," *PoS* **LATTICE2013** (2014) 371, arXiv:1311.0114 [hep-lat].

[24] **ALPHA** Collaboration, R. Höllwieser, F. Knechtli, and T. Korzec, "Scale setting for $N_f = 3 + 1$ QCD," *Eur. Phys. J. C* **80** no. 4, (2020) 349, arXiv:2002.02866 [hep-lat].

[25] M. Lüscher and S. Schaefer, "Lattice QCD with open boundary conditions and twisted-mass reweighting," *Comput. Phys. Commun.* **184** (2013) 519–528, arXiv:1206.2809 [hep-lat].

[26] **ALPHA** Collaboration, P. Fritzsch, R. Sommer, F. Stollenwerk, and U. Wolff, "Symanzik improvement with dynamical charm: a 3+1 scheme for Wilson quarks," *JHEP* **06** (2018) 025, arXiv:1805.01661 [hep-lat]. [Erratum: JHEP 10, 165 (2020)].

[27] R. Sommer, "A New way to set the energy scale in lattice gauge theories and its applications to the static force and alpha-s in SU(2) Yang-Mills theory," *Nucl. Phys. B* **411** (1994) 839–854, arXiv:hep-lat/9310022.

[28] M. Lüscher, "Properties and uses of the Wilson flow in lattice QCD," *JHEP* **08** (2010) 071, arXiv:1006.4518 [hep-lat]. [Erratum: JHEP 03, 092 (2014)].

[29] **APE** Collaboration, M. Albanese, F. Costantini, G. Fiorentini, F. Flore, M. Lombardo, R. Tripiccione, P. Bacilieri, L. Fonti, P. Giacomelli, E. Remiddi, M. Bernaschi, N. Cabibbo, E. Marinari, G. Parisi, G. Salina, S. Cabasino, F. Marzano, P. Paolucci, S. Petrarca, F. Rapuano, P. Marchesini, and R. Rusack, "Glueball Masses and String Tension in Lattice QCD," *Physics Letters B* **192** no. 1-2, (June, 1987) 163–169.

[30] A. Hasenfratz and F. Knechtli, "Flavor symmetry and the static potential with hypercubic blocking," *Phys. Rev. D* **64** (2001) 034504, arXiv:hep-lat/0103029.

[31] **ALPHA** Collaboration, M. Della Morte, S. Durr, J. Heitger, H. Molke, J. Rolf, A. Shindler, and R. Sommer, "Static quarks with improved statistical precision," *Nucl. Phys. B Proc. Suppl.* **129** (2004) 346–348, arXiv:hep-lat/0309080.

[32] M. Della Morte, A. Shindler, and R. Sommer, "On lattice actions for static quarks," *JHEP* **08** (2005) 051, arXiv:hep-lat/0506008.

[33] A. Grimbach, D. Guazzini, F. Knechtli, and F. Palombi, "O(a) improvement of the HYP static axial and vector currents at one-loop order of perturbation theory," *JHEP* **03** (2008) 039, arXiv:0802.0862 [hep-lat].

[34] M. Donnellan, F. Knechtli, B. Leder, and R. Sommer, "Determination of the Static Potential with Dynamical Fermions," *Nucl. Phys. B* **849** (2011) 45–63, arXiv:1012.3037 [hep-lat].

[35] **ALPHA** Collaboration, U. Wolff, "Monte Carlo errors with less errors," *Comput. Phys. Commun.* **156** (2004) 143–153, arXiv:hep-lat/0306017. [Erratum: Comput.Phys.Commun. 176, 383 (2007)].

[36] **ALPHA** Collaboration, S. Schaefer, R. Sommer, and F. Virotta, "Critical slowing down and error analysis in lattice QCD simulations," *Nucl. Phys. B* **845** (2011) 93–119, arXiv:1009.5228 [hep-lat].

[37] F. Joswig, S. Kuberski, J. T. Kuhlmann, and J. Neuendorf, "pyerrors: a python framework for error analysis of Monte Carlo data," arXiv:2209.14371 [hep-lat].

[38] A. Ramos, "Automatic differentiation for error analysis," *PoS* **TOOLS2020** (2021) 045, arXiv:2012.11183 [hep-lat].

[39] **TXL, T(X)L** Collaboration, G. S. Bali, B. Bolder, N. Eicker, T. Lippert, B. Orth, P. Ueberholz, K. Schilling, and T. Struckmann, "Static potentials and glueball masses from QCD simulations with Wilson sea quarks," *Phys. Rev. D* **62** (2000) 054503, arXiv:hep-lat/0003012.

[40] L. Struckmeier, R. Höllwieser, F. Knechtli, T. Korzec, M. Peardon, and J. A. Urrea-Niño, "Static-light meson spectroscopy with optimal distillation profiles," *PoS* **LATTICE2024** (2025) 104, arXiv:2501.12863 [hep-lat].